

FLOW MEASUREMENTS IN THE BORE OF A CARBON-DIOXIDE DRIVEN GEYSERING WELL

I. NURKAMAL¹, X. LU², A. WATSON² AND A.V. GORINE²

¹Lemigas, Indonesia

²Geothermal Institute, The University of Auckland, Auckland, New Zealand

SUMMARY – This paper presents measurements made in the bore of a well at Te Aroha in the North Island of New Zealand, and their interpretation. The well produces hot water and CO₂ from a production zone at a temperature of about 90°C, and discharges periodically like a geyser. Temperature surveys and pressure measurements at fixed depths have been made, allowing the determination of mean density and void fraction in the wellbore flow, leading to an understanding of the flow processes that govern the cyclic discharge.

1. INTRODUCTION

Te Aroha is a small town in the Waikato region of the North Island of New Zealand; it has natural geothermal springs and was a popular spa resort in the early 1900's. There are 3 geothermal wells, referred to as the Mokena geyser, the Wilson Street Bore and the Domain Trust Bore. The Mokena geyser was drilled in 1938. It has been left fully open to discharge naturally, which it does periodically like a geyser, and has become a local tourist feature. The water is collected for bathing facilities. Michels et al (1993) made measurements on the well and took samples, establishing that the major chemical component in the water is bicarbonate, with CO₂ in solution at a concentration of 3000 ± 500 mg/l at 60m below wellhead. The well is approximately 70m deep and has a maximum temperature of 90°C. The CO₂ comes out of solution during the passage of the water up the well. The output decreases over time due to calcite scale, and the well is reamed periodically to restore the cross sectional flow area.

The Wilson Street Bore and the Domain Trust bore are similar to the Mokena Geyser in their construction, discharge characteristics and fluid characteristics. The Wilson Street bore was chosen for these measurements because it is normally unused. It is 70m deep and cased almost to the bottom with 100mm bore casing.

The long-term objective of this work is to provide a better understanding of geysers, for scientific interest and to aid their preservation. Natural geysers are virtually impossible to make good flow experiments on, because of their natural flow passages. A literature review shows that the mechanism producing geysering flows may not be unique; some (Steinberg et al, 1981a,b) believe that it is necessary for there to be chambers in the flow path and a recharge route for shallow cold water to enter these. Others (Barth, 1950) suggest that the geysering is due solely to the fluid mechanics of the two-phase flow in a channel

with flow entering only at the bottom. The mechanics of geysering driven by the flashing of water will be different from that driven by ex-solution of gas. Ex-solution of gas in very long risers from seabed to production platforms is a topic of current interest to the petroleum industry. It has also been of interest in other industrial applications, see for example Griffiths (1962) and Kuncoro et al (1995).

2. INSTRUMENTATION AND MEASUREMENTS

2.1 Instrumentation

The temperature surveys were carried out with a chromel-alumel thermocouple lowered from the wellhead. The pressure measurements were carried out using a pair of Geokon vibrating wire piezometers- Figure 1 shows the arrangement.

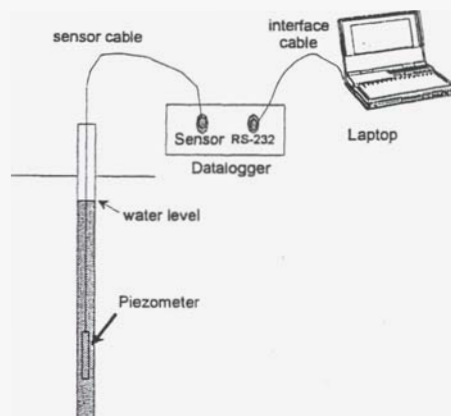


Figure 1: The arrangement of experimental equipment

The piezometers are 19.1mm in diameter and 133mm long, with surface readout. They

comprise a cylinder that is rigid except for a diaphragm that forms one end. Inside, a wire stretches down the axis from the rigid end to the centre of the diaphragm, so that if pressure outside the instrument varies, the diaphragm deflects and the wire tension changes. The wire can be plucked by an electromagnet; its natural frequency of vibration changes with tension, so a calibration allows natural frequency to be related to pressure outside the instrument. The frequency of vibration, in the range **2000-3000Hz**, is recorded in a datalogger at the surface. The instruments have a temperature limitation of 130°C , and a range of up to 10 bars. The accuracy is $\pm 0.02\%$ of full scale, or **20mm** water gauge.

To measure the steady state well discharge characteristics, a small cyclone separator was made from **PVC** pipe. The water flow rate from this was measured with a calibrated vessel and stopwatch. An attempt to measure the separated gas flow with a turbine flow-meter was unsuccessful because the gas was accompanied by very wet vapour that interfered with the electronics.

2.2 Well Discharge Characteristics

The well is normally left shut, when it has a wellhead pressure of 1-2 bar abs. depending on the effects of rainfall. When the well is discharging the aquifer pressure draws down and a significant change in output occurs after 1-2 days of continuous flow.

When the well was fully opened at the time of the measurements the average cycle period was 13 minutes. The flow rate into the well was then impossible to measure accurately, but was of the order of 0.35 kg/s .

2.3 Transient Pressure Measurements during Geysering

Shortly after the well was opened the water level in the well fell to approximately 6m below **CHF** during the geysering cycle. It was initially confirmed that the instruments were performing satisfactorily by hanging them together at the same depth, of just less than 6m so at minimum water level the instruments were recording above the water level. The differences were negligible in comparison to the overall pressure variation of 0.56 bar ($\approx 6\text{m}$ water gauge).

A series of measurements was then taken at various depths with one instrument 2m below the other. With the assumption of uniform radial pressure distribution this allowed the mean density and void fraction between the instruments to be determined.

3. RESULTS

After a discharge was finished, the water level fell and the well refilled, rising very steadily again to the wellhead. The steadiness of the start of overflow made it convenient to define this as the start of a cycle. This allowed the pressure variations through several successive cycles to be superimposed.

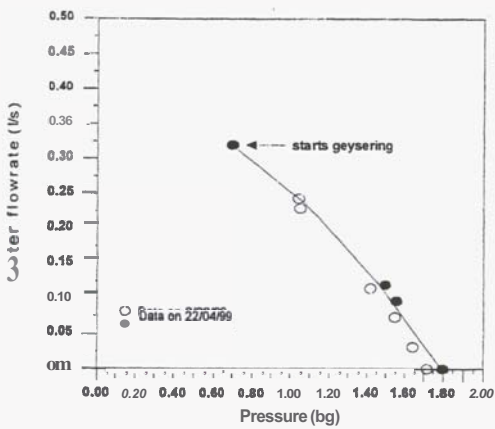


Figure 2: The **Wilson Street** bore discharge characteristic in steady flow

The discharge characteristic is shown in Fig 2, from which it can be seen that the well flows steadily until the wellhead pressure falls to **0.7 bar**. When opened further cycling begins.

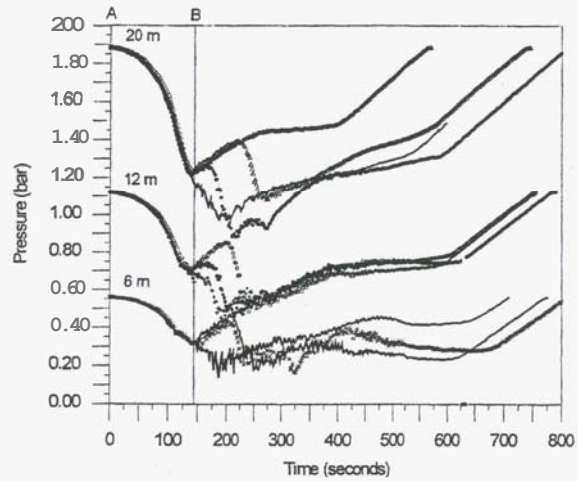


Figure 3: The pressure variations measured at various depths for the geysering cycle

Fig. 3 shows three superimposed cycles with instruments at 6 and 12m and four cycles with it at **20m** from which it can be seen that: -

- the pressure reduction immediately after the start (A-B or **0-140** seconds) is very consistent from cycle to cycle
- the middle part of the cycle from 140-500 seconds is erratic
- the cycles are not of equal period but show a variation of $\pm 6\%$
- the end part of the cycle shows a linear variation of pressure with time corresponding to a water level that rises at constant velocity of about **0.025m/s**

Pressure measurements at **20m** depth have a similar shape but show much smaller fluctuations in the middle part of the cycle.

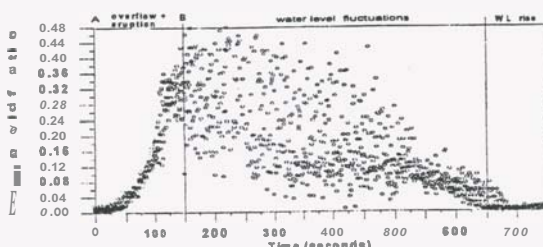


Figure 4: The mean void fraction during geysering cycles at nominal depth of 7m

Fig 4 shows the void fraction at a nominal depth of 7m, from which it can be deduced that at the end of the cycle any bubbles in the fluid are small enough and far enough apart not to affect the density - i.e. the water refilling the empty part of the well is virtually gas free. At the beginning of the cycle (A-B), the bubbles present in the well from 7m to wellhead increase regularly with time in a non-linear manner.

4. INTERPRETATION OF RESULTS

In order to grasp the main feature of the geysering cycles, two figures have been generated to interpret the physical process of the cyclic eruptions in Wilson Street Bore (Lu and Watson, 2001).

A typical pressure-time curve for **20m** depth is shown in Figure 5. In this Figure, the pressure and time is based on the averaged value of the four cycles in Figure 3.

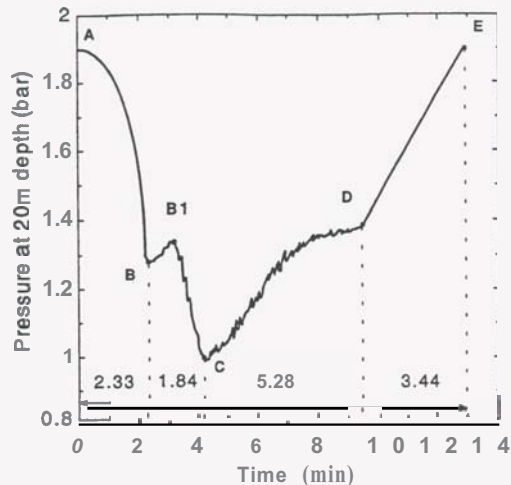


Figure 5: A typical pressure-time curve at 20m depth used for the interpretation

Based on the experimental data of solubility of CO_2 in water and the relevant correlations (Malinin, 1974; Ellis and Golding, 1963; Alkan et al., 1995), and using the concentrations in the Mokona geyser estimated by Michels et al (1993), the depth at which gas first comes out of solution (flash point) has been estimated. It is found that the flash point varies throughout the cycle. This and the water level estimated from the measurements are shown in Figure 6, which illustrates a picture of the physical processes leading to the geysering action.

The whole cycle can be broken into **4** stages. The detailed interpretations of each stage are as follows.

Process A-B: from overflow to eruption

State A indicates the start of the geysering cycle when the water just reaches the top of the well and overflows. Before overflow, the solution in the well is at equilibrium state. As soon as it overflows, the equilibrium is broken due to the smooth decrease of hydrostatic pressure (overflow on the top of the well), which causes CO_2 gas release from the solution. As more and more bubbles form in the well, the void fraction increases and the hydrostatic pressure decreases at different depths, resulting in more CO_2 gas coming of solution. The bubble growth is very fast due to this rapid chain reaction along the well.

This is a transient two-phase flow process. From A to B, transition occurs from bubbly flow to slug flow. After **2.33** min (at B), the upper **20m** of the well is filled by Taylor bubbles with void fraction $> 30\%$ causing eruptions at well head. Note that the curve from A to B in Figure 3 looks very smooth and the curves of the individual cycles almost overlap from A to B, which is an important characteristic of this process.

In Figure 6, the flash point at time A is about 55m depth from the well head; that is 15m above the bottom (the well is 70m deep). In this case, the solution in the bottom **15m** is still at entirely liquid, without release of **CO₂ gas** to form bubbles. From A to B, the flash point is moving deeper in the well. Because of the decrease in hydrostatic pressure, more gas is liberated.

Process B-C: Eruptions with different vigour

Eruptions occur from B to **C**. This process lasts nearly 2 minutes (**1.84** minutes in Figure 5). The pressure at B1 is greater than that at B, which can be explained **as** follows.

Because the gas distribution along the well is not uniform, after the eruption at B, the void fraction in the upper **20m** of the column that causes the pressure at 20m depth to increase, at B1. After B1, more big bubbles rise into the upper 20m. They coalesce and form slug flow with void fraction of about 37%, causing bigger eruptions, at C, which corresponds to the lowest pressure measured at 20m. Note that curve **B-C** in Figure 5, is not smooth due to the different vigorous eruptions causing pressure variations at 20m depth. The bubble behaviour is less regular.

The flash point at C is at its lowest level in the well, only about 2m above the bottom. This indicates that almost all the solution in the well has contributed to releasing CO₂ **gas** in the well.

Process C-D: Water level falls and fluctuates

At time C, **4.17** minutes have elapsed since time A, much of the CO₂ **gas** has been released from

the solution. The inflow at the bottom of the well is so slow (inflow velocity is only about 0.025 m/s) that it cannot supply enough gas to match the departure **from** the top **as** slugs. This can be concluded from Figure 6 in which the reference element RE, rising at uniform velocity, is below the flash point curve at all times between **C** and **E**. The dissolved gas supply is insufficient to maintain the void fraction in the well at its earlier levels. A small value of void fraction means small volume of the fluid in the well, and the water level in the well falls (see the water level curve in Figure 6). In other words, the gas in the slugging part of the well travels to the exit faster than the liquid. In this part of the cycle a decreasing part of the column is filled with **gas** that can produce gas – the flash level is moving upwards. There is a smaller length of unsteady upward two-phase flow and the water level fluctuations decrease **as** a result. At D, after 5.28 minutes, the remaining gas bubbles in the well have almost all been released and the void fraction is close to zero.

In **summary**, the combination of the slip between liquid and gas in the upper part of the well, the variation in flash point level and the steady inflow at the bottom results in the water level dropping to about 5m below wellhead at D, while the pressure at 20m depth increases steadily but non-linearly **from C to D**. The water level fluctuates during this period.

Process D-E: Water level rises

After D, the fluid in the well is almost pure liquid, although there may be very small bubbles spaced so that they do not affect the hydrostatic pressure. No new **CO₂ gas** comes out solution because the

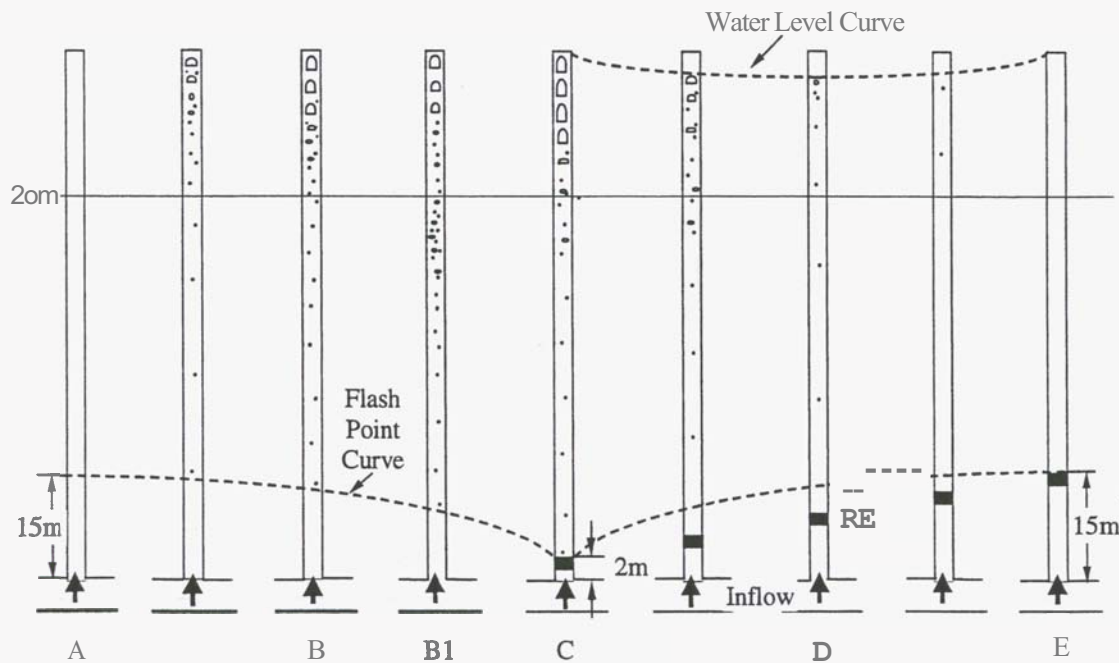


Figure 6: **Schematic diagram** of the physical processes in the well leading to the geysering cycles

hydrostatic pressure increases with time at all depths below water level. The water level rises at constant speed (graph D-E is almost linear) until it reaches the wellhead at E. After E, another cycle starts again. It is likely that the flow rate from the aquifer into the well varies in accordance with variations in hydrostatic pressure at the production depth, but these variations will be small enough to affect the interpretation of events.

5. FURTHER STUDY

Additional measurements in the well are being planned. A Nitrogen Gas Purge System has been selected to measure the pressure variations at different depths of the well simultaneously. These measurements should provide enough information to test a computational model of the flow in the well that is being developed. From this, an examination of the flow processes in true geysers driven by water and steam will be undertaken. It is almost impossible to make measurements on natural geysers because of their geometry. Measurements in geysering wells such as those presented here may provide the best approach to gaining the level of understanding necessary to be able to analyse the effect of variations in aquifer conditions on geyser behaviour and hence preserve geysers.

6. CONCLUSIONS

The flow measurements have been carried out on the carbon dioxide driven geysering well known as the Wilson Street Bore at Te Aroha. The measurements allow the physical processes during the geysering cycle to be determined qualitatively. The geysering in the well is due solely to the fluid mechanics of the two-phase flow in the wellbore. This supports the suggestion made by Barth (1950) that geysering can occur due to the fluid mechanics of the flow passage alone, and it is not essential that there be chambers and separate flows of hot and cold water. There is, of course, no evidence from these measurements to exclude the latter as contributing to a possible geysering mechanism.

7. ACKNOWLEDGEMENTS

Iman Nurkamal was supported by a scholarship provided by the New Zealand Ministry of Foreign Affairs and Trade as part of its Overseas Development Assistance Programme.

8. REFERENCES

Alkan, H., Babadagli, T., and Satman, A. (1995). The prediction of PVT/phase behavior of the geothermal fluid mixtures. *Proceedings of World Geotherm Congress*, vol. 3, pp. 1659-1665.

Barth, T. F. W. (1950). Volcanic Geology Hot springs and Geysers of Iceland. *Publication 587, Carnegie Institution of Washington*.

Ellis, A. J., and Golding, R. M. (1963). The solubility of carbon dioxide above 100°C in water and in sodium chloride solutions. *American Journal of Science*, Vol. 261, p. 47

Griffith, P. (1962), Geysering in liquid-filled lines. *ASME-AIChE Heat Transfer Conference, Paper 62-HT-39*.

Kuncoro, H., Rao, Y. F. and Fukuda, K. (1995), An experimental study on the mechanism of geysering in a closed two-phase thermosyphon. *Int. Jnl. Multiphase Flow, Vol 21, No.6, pp.1243-1252*.

Lu X. and Watson, A. (2001). Interpretation of the Measurements of a Geysering Well at Te Aroha. *Proceedings of 8th NZ Engineering and Technology Postgraduate Student Conference 2001*, Hamilton, New Zealand.

Malinin, S. D. (1974). Thermodynamics of the H₂O-CO₂ system. *Geochemistry International*, Vol. 11, pp. 1060-1085.

Michels, D. E., Jenkinson, D. and Hochstein, M. P. (1993). Discharge of thermal Fluids at Te Aroha (NZ), *Proceedings 15th NZ Geothermal Workshop 1993. Auckland, New Zealand*, pp.21-27

Steinberg, G. S., Merzhanov, A. G. and Steinberg, A. S. (1981a). Geyser Process: Its Theory, Modeling, and Field Experiment. Part 1. Theory of the geyser Process. *Modern Geology, Vol.8, pp. 67-70*

Steinberg, G. S., Merzhanov, A. G. and Steinberg, A. S. (1981b). Geyser Process: Its Theory, Modeling, and Field Experiment. Part 2. A laboratory model of a geyser. *Modern Geology, Vol.8, pp. 71-74*